Energy Management System for Hybrid Electrical Vehicle Using a Bidirectional DC/DC Converter Topology

*1Dharmireddy Mani ,2Kondapalli Papa Rao
M. Tech Scholar, Department of EEE,KIET-II, Kakinada,A.P,India.[1]
Asst.Professor Department of EEE,KIET-II, Kakinada, A.P, India.[2]
Corresponding Author:- *dharmireddymani1998@gmail.com

ABSTRACT

This paper organizes applications for a hybrid electric vehicle system operating on a main energy store (ES1), an auxiliary energy store (ES2), and a new bidirectional DC-DC converter (BDC) that connects different DC buses. Voltage level. The proposed BDC converter can be operated in both step-up and step-down modes. In step-up mode, which represents low-voltage dual-source power mode, and step-down mode, which represents high-voltage DC link energy recovery mode, both modes operate under the control of bidirectional power flow. This model can independently control the power flow between low voltage dual source back / boost modes. Described here are circuit configuration, operation, steady-state analysis, and proposed BDC tuning for the three transmission modes. A fuzzy logic controller is used in this project, and system results are also verified by MATLAB / SIMULINK software. Index Term- Bidirectional DC / DC Converter (BDC), Dual Battery Storage, Hybrid Electric Vehicle, Fuzzy Logic Controller. I. INTRODUCTION Changes in the global environment and reduced energy supply have changed vehicle innovation. Advanced technologies are currently being investigated for future vehicle applications. Among these applications, fuel cell hybrid electric vehicles (FCV / HEV) are efficient and promising candidates. Formerly Ehsani et al. Vehicle dynamics were investigated to find the optimum torque-velocity profile for electric drive systems [1]. Emadietal. He talked about regional operating characteristics of various vehicles, including HEVs, FCVs, and other electric vehicles. [2] Emadi et al. To deal with huge vehicle loads. It is also an integrated power electronics intensive solution [3]. Schaltz et al. It adequately distributes load power among fuel cell stacks, batteries, and ultracapacitors based on the two proposed energy management strategies [4]. Thounthong et al. We investigated the effects of fuel cell (FC) design and the benefits of control system hybridization [5]. Chan et al. Investigated electric vehicles, hybrid vehicles, and fuel cell vehicles, focusing on the structure and modeling of energy management [6]. Khaligh and Li have introduced energy storage topologies for HEVs and plug-in HEVs (PHEVs). We also analyzed and compared batteries, UC and FC technologies. We also considered various hybrid ESSs that integrate two or more storage devices [7]. Rajashekara talked about flow conditions and the need for key electrical drive components, batteries, electric motors, and power electronics [8]. He implemented a bidirectional DC / DC converter topology with Rye et al. Two-stage and nested quality. The voltage ratio of the converter has been improved in EV and DC microgrid systems. Lai also investigated a bidirectional DC-DC converter (BDC) topology with a high voltage conversion ratio for EV batteries in combination with a DC microgrid system [10]. In FCV systems, primary batteries are typically used to start the FC and power the drive motor [2, 3]. The battery storage system improves the inherently slow response time of the FC stack by providing peak power when the vehicle accelerates [7]. It also includes high power density components such as supercapacitors (SCs) that eliminate peak power transients during acceleration and regenerative braking [11]. In general, SCs can store renewable energy when decelerating and release it again when accelerating, thus providing additional power. The high power density of the SC extends the life of stacked FC and battery storage devices and improves the overall efficiency of FCV systems. This study suggests a nested voltage doubler structure [9, 28] and a synchronous buck-boost circuit. These are two new BDC topologies for FCV / HEV power systems. It focuses on two main modes of operation: low voltage dual source power supply mode and high voltage DC bus energy recovery mode. In addition, when the converter is in low voltage dual source buck-boost mode, the proposed converter can independently control the power flow between any two low voltage sources. A similar topology is shown in [29], but this only describes a simple idea. Meanwhile, this study provides a detailed analysis of the behavior and regulation of this new topology, as well as simulation results for all modes of operation. The proposed converter extends the topology shown in [29] in this study because it can operate over a wider voltage range. The main characteristics of the proposed converter can be summarized as follows. ¬ Connect three or more DC power supplies with different voltage levels. ¬ Controls the flow of power between the DC bus and the two low voltage sources. Increases power flow between the two low voltage sources, static voltage boost, and reduces voltage stress on the switch. ¬ It has a reasonable duty cycle and creates a wide voltage difference between the high side port and the low side port. A functional diagram of a typical (FCV / HEV) power supply system is shown in Figure 1 [4, 13]. The low voltage FC stack is used as the main power supply and the SC is connected directly in parallel with the FC. The DC / DC power converter is used in the drive inverter to convert the FC stack voltage to a sufficient DC bus voltage to power the drive motor. In addition, a fairly high voltage ES1 can be used as main battery storage to provide peak power, and a fairly low voltage ES2 can be used as auxiliary battery storage to realize the concept of a vehicle range extender [13]. .. The function of the bidirectional DC / DC converter (BDC) is to connect the dual battery energy storage device to the DC bus of the drive inverter. Generally, the voltage levels of the FC stack and battery storage are different. Several multiport BDCs have been developed to provide a specific voltage to the load and control the flow of power between different sources. This reduces overall cost, mass, and power consumption [1427]. These BDCs can be divided into isolated and non-isolated types.

High frequency power transformers are used in isolated converters to enable galvanic insulation. Several isolated multiport BDC topologies are being investigated, including flyback, half or full bridge circuits, dual active bridges, and resonant circuits. The literature suggests that non-separated BDCs are more effective than typical isolated BDCs for EVs. Liu et al. The combination of Buck, Boost, Ćuk, and Sepic inferred a non-isolated multi-input converter topology. [23] Wu et al. We have developed a non-isolated multi-input, multi-output (MIMO) converter topology with three ports for connecting renewable energy sources, batteries, and loads simultaneously. The three double-input converters developed in [19] consist of a single-pole triple slow switch and only one inductance.

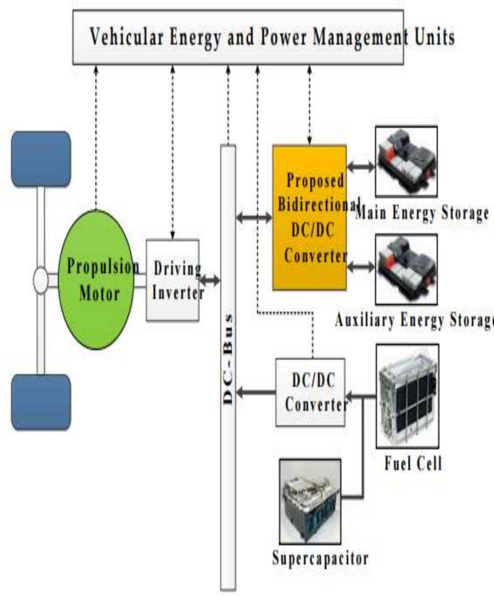

Fig.1.Typical functional diagram for a FCV/HEV power system.

A modular, non-separable MIMO converter has been announced. This converter is used to hybridize clean energy sources from electric vehicles, with basic boost circuitry modified and integrated. However, the voltage gain of MIMO boost circuits is actually limited due to the loss associated with some components such as mains switches, inductors, filter capacitors, and rectifier diodes.

To overcome this shortcoming, a 3-port high gain power converter was introduced that included an FC, battery source, stack output for connecting HEVs, and a DC microgrid. The multi-port BDC described can connect three or more power supplies and operate at different voltage levels, but the limited static voltage gain narrows the voltage range and between the high-side and low-side ports. The voltage difference becomes smaller.

II. Recommended Topology

The proposed BDC topology with double battery energy storage is shown in Figure 1. Here, VH,

VES1, and VES2 have two bidirectional power switches (SES1 and SES2) in a high voltage intermediate circuit voltage, main energy storage (ES1), and auxiliary energy storage (system ES2), or converter structure. Use to turn the ES1 and ES2 current loops on and off. The charge pump capacitor (CB) features four active switches (Q1, Q2, Q3, Q4) and two phase inductors (L1, L2) to improve static voltage amplification between the two low voltage doubles. The high voltage DC (VH) bus of the source (VES1, VES2.)) And the proposed converter is integrated as a voltage divider. In addition, the additional CB reduces the
switch voltage load on the active switch, eliminating the need for extreme duty cycle operations. In addition, the three bidirectional power switches (S, SES1, SES2) shown in Figure 2 operate in four quadrants, controlling the power flow between the two low-voltage dual power supplies (VES1, VES2), and one of them. Is used to block. Positive or negative voltage.

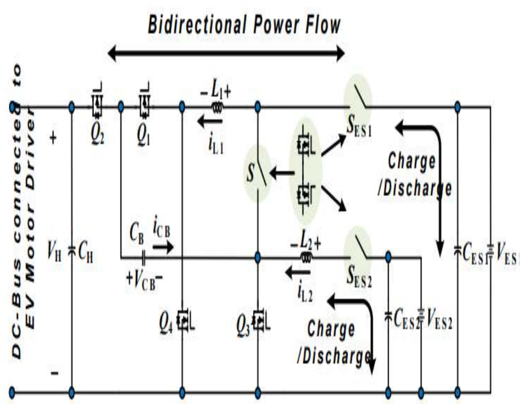

Fig.2.1. Proposed BDC topology with dual-battery energy storage.

This bidirectional power switch is implemented via two metal-oxide-semiconductor field-effect transistors (MOSFETs), pointing in opposite directions, in series connection. To explain the concept for the proposed converter, all the conduction statuses of the power devices involved in each operation mode are displayed in Table 2.1. Accordingly, the four operating modes are illustrated as follows to enhance understanding.

TABLE 2.1.

CONDUCTION STATUS OF DEVICES FOR DIFFERENT OPERATING MODES

Operating Modes	ON	OFF	Control Switch	Synchronous Rectifier (SR)
Low-voltage dual-source-powering mode (Accelerating, $x_1=1, x_2=1$)	S_{ES1}, S_{ES2}	S	Q_3, Q_4	Q_1, Q_2
High-voltage dc-bus energy-regenerating mode (Braking, $x_1=1, x_2=1$)	S_{ES1}, S_{ES2}	S	Q_1, Q_2	Q_3, Q_4
Low-voltage dual-source buck mode (ES1 to ES2, $x_1=0, x_2=0$)	S_{ES1}, S_{ES2}	Q_1, Q_2, Q_4	S	Q_3
Low-voltage dual-source boost mode (ES2 to ES1, $x_1=0, x_2=0$)	S_{ES1}, S_{ES2}	Q_1, Q_2, Q_4	Q_3	S
System shutdown	--	S_{ES1}, S_{ES2} Q_1, Q_2, Q_3, Q_4	--	--

2.1. Low-Voltage Dual-Source-Powering Mode

Fig. 2.2(a) depicts the circuit schematic and steady-state wave forms for the converter under the low-voltage dual-source-powering mode. Therein, the switch S is turned off, and the switches (SES1, SES2) are turned on, and the two low-voltage dual sources (VES1, VES2) are supplying the energy to the dc-bus and loads. In this mode, the low-side switches Q3 andQ4 are actively switching at a phase-shift angle of 180°, and the high-side switches Q1 and Q2 function as the synchronous rectifier (SR). Based on the typical waveforms shown in Fig. 2.2(b), when the duty ratio is larger than 50%, four circuit states are possible (Fig. 2.2). In the light of the on/off status of the active switches and the operating principle of the BDC in low-voltage dual-source-powering mode, the operation can be explained briefly as follows.

State 1 [t0 < t < t1]: During this state, the interval time is (1-Du)Tsw, switches Q1, Q3 are turned on, and switches Q2, Q4 are turned off. The voltage across L1 is the difference between the low-side voltage VES1 and the charge-pump voltage (VCB), and hence iL1 decreases linearly from the initial value. In addition, inductor L2 is charged by the energy source VES2,

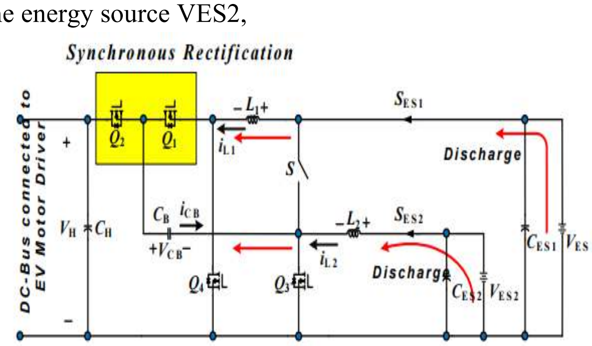

(a)

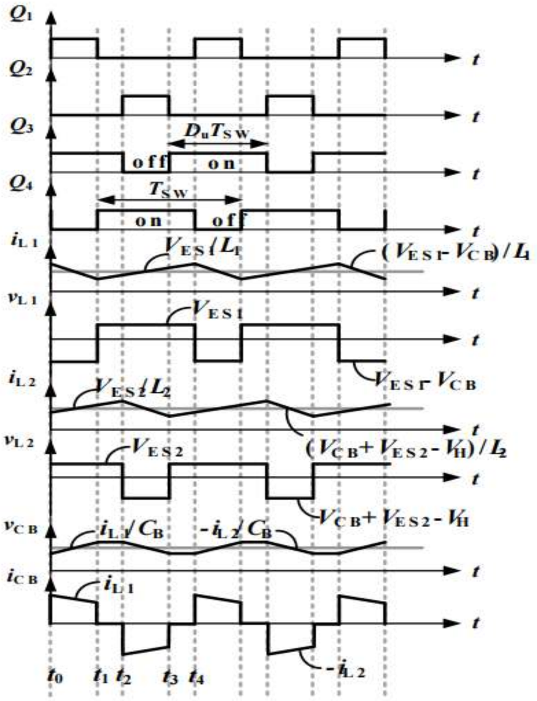

(b)

Fig. 2.2. Low-voltage dual-source-powering mode of the proposed BDC: (a)
circuit schematic and (b) steady-state waveforms.

thereby generating a linear increase in the inductor current. The voltages across inductors L1 and L2 can be denoted as

$$L_1 \frac{di_{L1}}{dt} = V_{ES2} - V_{CB} \qquad (1)$$

$$L_2 \frac{di_{L2}}{dt} = V_{ES2} \qquad (2)$$

State 2 [t1 < t < t2]: During this state, the interval time is (Du-0.5)Tsw; switches Q3 and Q4 are turned on; and switches Q1 and Q2 are turned

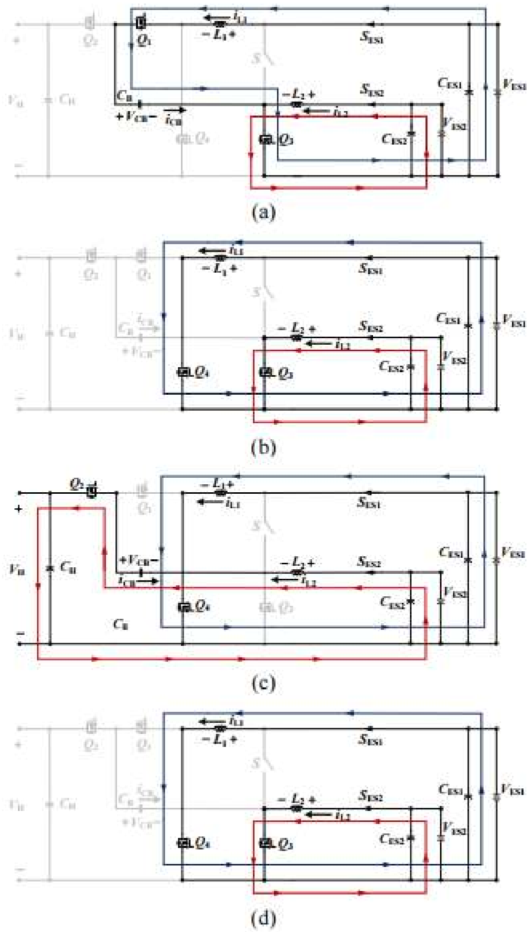

Fig. 2.3 Circuit states of the proposed BDC for the low-voltage
dual-source-powering mode. (a) State 1. (b) State 2. (c) State 3. (d) State 4.

a) off. The low-side voltages VES1 and VES2 are located between inductors L1 and L2, respectively, thereby linearly increasing the inductor currents, and initiating energy to storage. The voltages across inductors L1 and L2 under state 2 can be denoted as

$$L_1 \frac{di_{L1}}{dt} = V_{ES1} \qquad (3)$$

$$L_2 \frac{di_{L2}}{dt} = V_{ES2} \qquad (4)$$

b) State 3 [t2 < t < t3]: During this state, the interval time is (1-Du)Tsw; switches Q1 and Q3 are turned on, whereas switches Q2 and Q4 are turned off. The voltages across inductors L1 and L2 can be denoted as

$$L_1 \frac{di_{L1}}{dt} = V_{ES1} \quad (5)$$

$$L_2 \frac{di_{L2}}{dt} = V_{CB} + V_{ES2} - V_H \quad (6)$$

c)State 4 [t3< t <t4]: During this state, the interval time is (Du-0.5)Tsw; switches Q3 and Q4 are turned on, and switches Q1 and Q2 are turned off. The voltages across inductors L1 and L2 can be denoted as

$$L_1 \frac{di_{L1}}{dt} = V_{ES1}$$

$$L_2 \frac{di_{L2}}{dt} = V_{ES2}$$

2.2. High-Voltage DC-Bus Energy-Regenerating Mode :

In this mode, the kinetic energy stored in the motor drive is fed back to the source during regenerative braking operation. The regenerative power can be much higher than what the battery can absorb. Consequently, the excess energy is used to charge the energy storage device. The circuit schematic and the steady-state waveforms of the BDC under the high-voltage dc bus energy-regenerating mode are illustrated in Fig.2.4.

Therein, the current in the inductors is controlled by the active switches Q1 and Q2, which have a phase-shift angle of 180° and thereby direct the flow away from the dc-bus and toward the dual energy storage devices; the switches Q3 and Q4 function as the SR to improve the conversion efficiency.

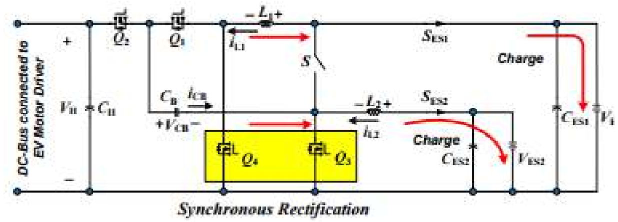

(a)

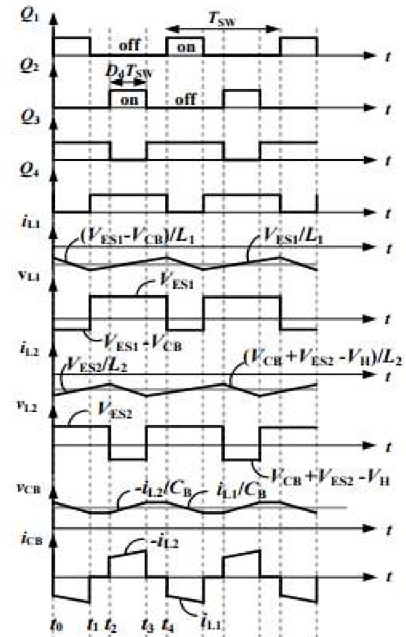

(b)

Fig.2.4. High-voltage dc-bus energy-regenerating mode of the proposed BDC: (a) circuit schematic and (b) steady-state waveforms.

On the basis of the steady-state waveforms shown in Fig. 2.4(b), when the duty ratio is below 50%, four different circuit states are possible, as shown in Fig. 2.5. In the light of the on-off status of the active switches and the operating principle of the BDC in high-voltage dc-bus energy-regenerating mode, the operation can be depicted briefly as follows.

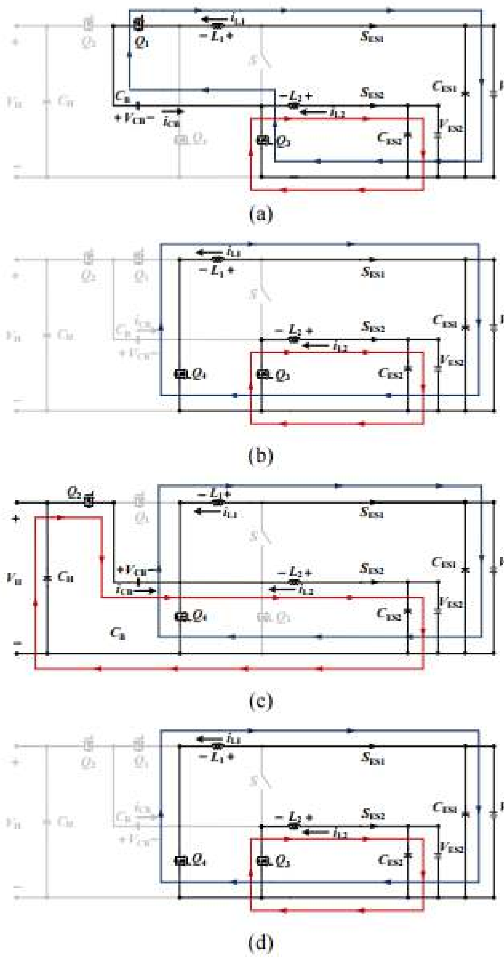

Fig. 2.5. Circuit states of the proposed BDC for the high-voltage dc-bus energy-regenerating mode. (a) State 1. (b) State 2. (c) State 3. (d) State 4.

a) State 1 [t0 < t < t1]: During this state, the interval time is Dd Tsw; switches Q1 and Q3 are turned on, and switches Q2 and Q4 are turned off. The voltage across L1 is the difference between the low-side voltage VES1 and the charge-pump voltage VCB; hence, the inductor current iL1 decreases linearly from the initial value. In addition, inductor L2 is charged by the energy source VES2, which also contributes to the linear increase in the inductor current. The voltages across inductors L1 and L2 can be denoted as

$$L_1 \frac{di_{L1}}{dt} = V_{ES1} - V_{CB} \tag{9}$$

$$L_2 \frac{di_{L2}}{dt} = V_{ES2} \tag{10}$$

b) State 2 [t1 < t < t2]: During this state, the interval time is (0.5-Dd)Tsw; switches Q3 and Q4 are turned on, and switches Q1and Q2 are turned off. The voltages across inductors L1 and L2 are the positive the low-side voltages VES1 and VES2, respectively; hence, inductor currents iL1 and iL2 increase linearly. These voltages can be denoted as

$$L_1 \frac{di_{L1}}{dt} = V_{ES1} \tag{11}$$

$$L_2 \frac{di_{L2}}{dt} = V_{ES2} \tag{12}$$

c) State 3 [t2 < t < t3]: During this state, the interval time is DdTsw; switches Q1 and Q3 are turned off, and switches Q2 and Q4 are turned on. The voltage across L1 is the positive low-side voltage VES1 and hence iL1 increases linearly from the initial value. Moreover, the voltage across L2 is the difference of the high-side voltage VH, the charge-pump voltage VCB, and the low-side voltage VES2, and its level is negative. The voltages across inductors L1 and L2 can be denoted as

$$L_1 \frac{di_{L1}}{dt} = V_{ES1} \tag{13}$$

$$L_2 \frac{di_{L2}}{dt} = V_{ES2} + V_{CB} - V_H \tag{14}$$

d) State 4 [t3 < t < t4]: During this state, the interval time is (0.5-Dd)Tsw; switches Q3 and Q4 are turned on, and switches Q1 and Q2 are turned off. The voltages across inductors L1 and L2 can be denoted as

$$L_1 \frac{di_{L1}}{dt} = V_{ES1} \tag{15}$$

$$L_2 \frac{di_{L2}}{dt} = V_{ES2} \tag{16}$$

Remaining modes of operation were explained in [1].

3. FUZZY CONTROLLER:

The word Fuzzy means vagueness. Fuzziness occurs when the boundary of piece of information is not clear-cut. In 1965 Lotfi A. Zahed propounded the fuzzy set theory. Fuzzy set theory exhibits immense potential for effective solving of the uncertainty in the problem. Fuzzy set theory is an excellent mathematical tool to handle the uncertainty arising due to vagueness. Understanding human speech and recognizing handwritten characters are some common instances where fuzziness manifests.

Fuzzy set theory is an extension of classical set theory where elements have varying degrees of membership. Fuzzy logic uses the whole interval between 0 and 1 to describe human reasoning. In FLC the input variables are mapped by sets of membership functions and these are called as "FUZZY SETS".

Fuzzy set comprises from a membership function which could be defines by parameters. The value between 0 and 1 reveals a degree of membership to the fuzzy set. The process of converting the crisp input to a fuzzy value is called as "fuzzificaton." The output of the Fuzzier module is interfaced with the rules. The basic operation of FLC is constructed from fuzzy control rules utilizing the values of fuzzy sets in general for the error and the change of error and control action. Basic fuzzy module is shown in fig.5

The results are combined to give a crisp output controlling the output variable and this process is called as "DEFUZZIFICATION."

4.1 MATLAB CIRCUITS:

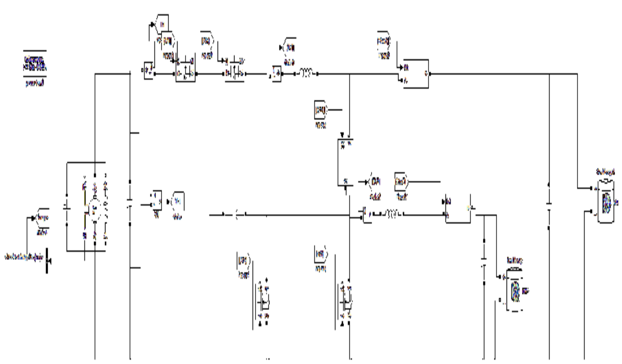

Fig4.1 Simulation Block Diagram

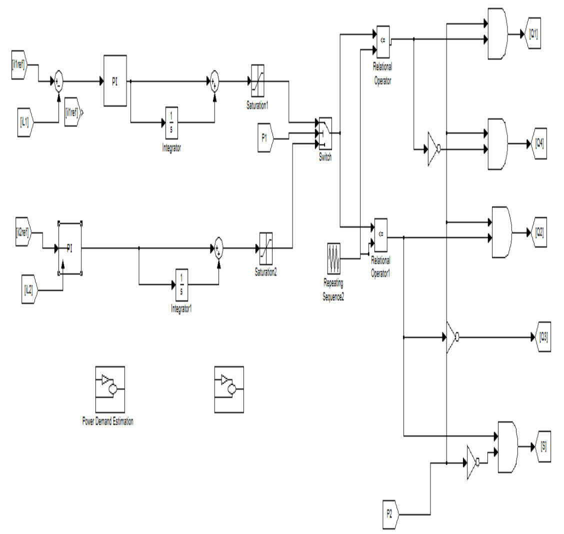

Fig4.2 Simulation Control Diagram

4.2 WAVE FORMS:

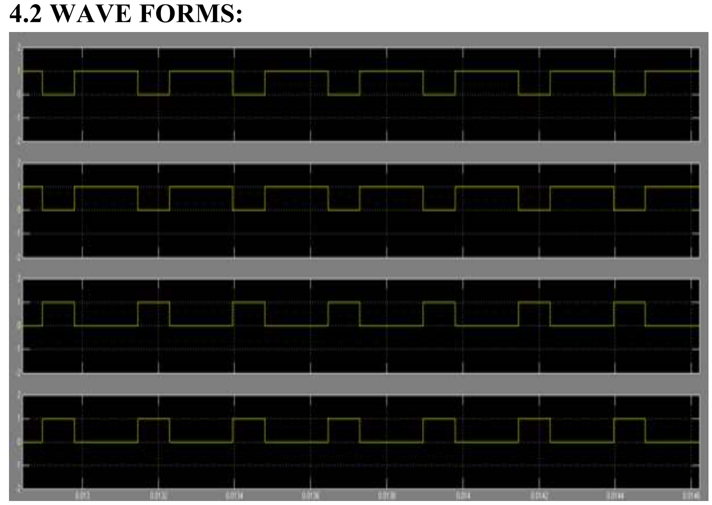

Fig. 4.3. Measured waveforms for low-voltage dual-source-powering mode:(a) gate signals

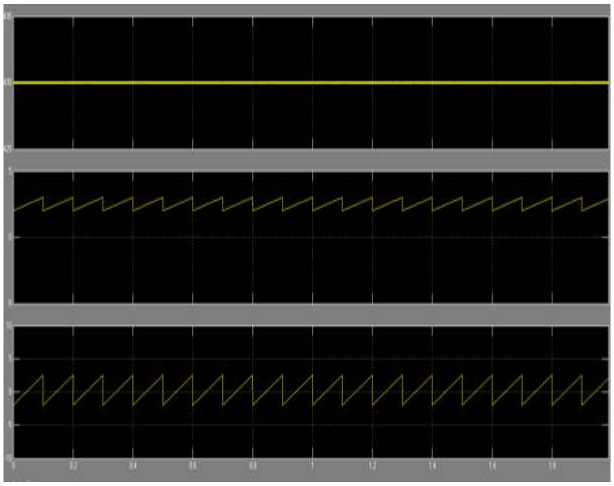

(b) output voltage and inductor currents.

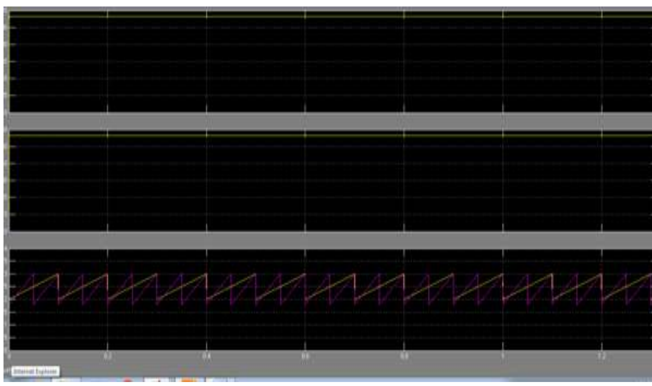

Fig. 4.4. Measured waveforms for high-voltage dc-bus energy-regenerating mode:.

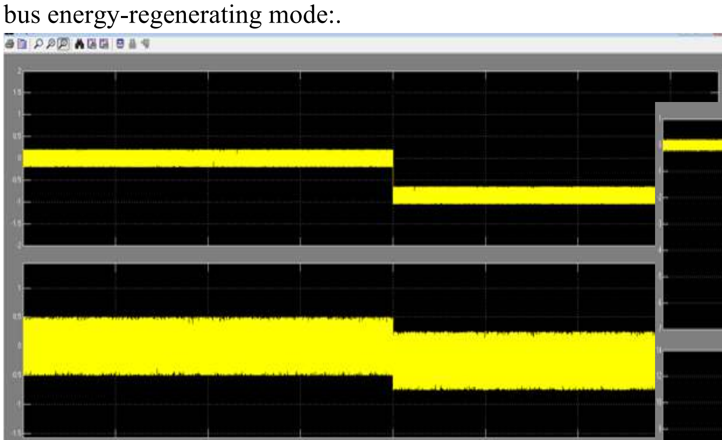

Fig.4.5. Waveforms of controlled current step change in the low-voltage dual-source-powering mode by simulation

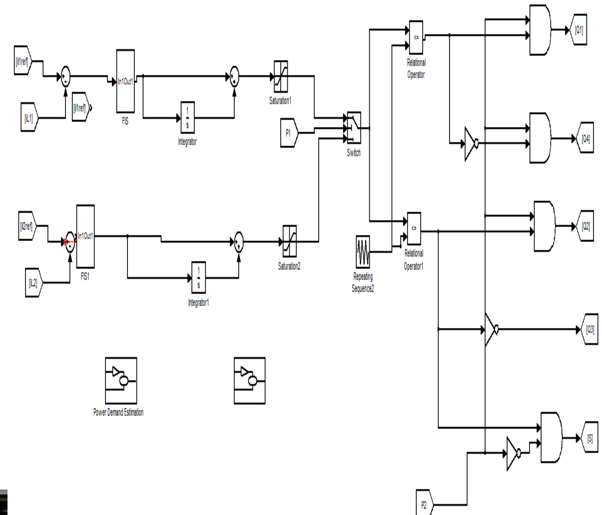

Fig4.6 Simulation of fuzzy logic Control Diagram

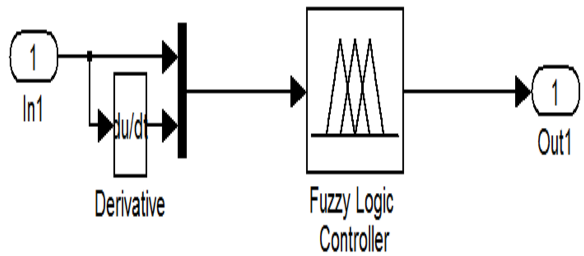

Fig4.7 fuzzy logic Controller

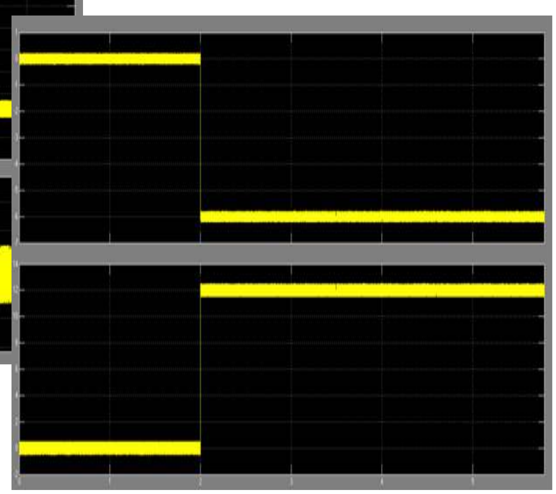

Fig. 4.8 Waveforms of controlled current step change in the low-voltage dual-source boost mode: by simulation;

Fig. 4.9 Waveforms of controlled current step change in the low-voltage dual- source buck mode: by simulation

CONCLUSION

A new BDC topology was presented to interface dual battery energy sources and high-voltage dc bus of different voltage levels. The circuit configuration, operation principles, analyses, and static voltage gains of the proposed BDC were discussed on the basis of different modes of power transfer. Simulation waveforms for a 1 kW prototype system highlighted the performance and feasibility of this proposed BDC topology. The highest conversion efficiencies were 97.25%, 95.32%, 95.76%, and 92.67% for the high-voltage dc-bus energy-regenerative buck mode, low-voltage dual-source-powering mode, low-voltage dual-source boost mode (ES2 to ES1), and low-voltage dual-source buck mode (ES1 to ES2), respectively. In this paper fuzzy logic controller is used to enhance the proposed topology. The results demonstrate that the proposed BDC can be successfully applied in FC/HEV systems to produce hybrid power architecture.

REFERENCES

[1] Ching-Ming Lai, Member, IEEE, Yu-Huei Cheng, Senior Member, IEEE, Ming-Hua Hsieh, and Yuan-Chih Lin” Development of a Bidirectional DC/DC Converter with Dual-Battery Energy Storage for Hybrid Electric Vehicle System” 2017 IEEE

[2] M. Ehsani, K. M. Rahman, and H. A. Toliyat, "Propulsion system design of electric and hybrid vehicles," IEEE Transactions on industrial electronics, vol. 44, no. 1, pp. 19-27, 1997.

[3] A. Emadi, K. Rajashekara, S. S. Williamson, and S. M. Lukic, "Topological overview of hybrid electric and fuel cell vehicular power system architectures and configurations," IEEE Transactions on Vehicular Technology, vol. 54, no. 3, pp. 763-770, 2005.

[4] A. Emadi, S. S. Williamson, and A. Khaligh, "Power electronics intensive solutions for advanced electric, hybrid electric, and fuel cell vehicular power systems," IEEE Transactions on Power Electronics, vol. 21, no. 3, pp. 567-577, 2006.

[5] P. Thounthong, V. Chunkag, P. Sethakul, B. Davat, and M. Hinaje, "Comparative study of fuel-cell vehicle hybridization with battery or supercapacitor storage device," IEEE transactions on vehicular technology, vol. 58, no. 8, pp. 3892-3904, 2009.

[6] C. C. Chan, A. Bouscayrol, and K. Chen, "Electric, hybrid, and fuel-cell vehicles: Architectures and modeling," IEEE transactions on vehicular technology, vol. 59, no. 2, pp. 589-598, 2010.

[7] A. Khaligh and Z. Li, "Battery, ultracapacitor, fuel cell, and hybrid energy storage systems for electric, hybrid electric, fuel cell, and plug-in hybrid electric vehicles: State of the art," IEEE transactions on Vehicular Technology, vol. 59, no. 6, pp. 2806-2814, 2010.

[8] K. Rajashekara, "Present status and future trends in electric vehicle propulsion technologies," IEEE Journal of Emerging and Selected Topics in Power Electronics, vol. 1, no. 1, pp. 3-10, 2013.

[9] C.-M. Lai, Y.-C. Lin, and D. Lee, "Study and implementation of a two-phase interleaved bidirectional DC/DC converter for vehicle and dc-microgrid systems," Energies, vol. 8, no. 9, pp. 9969-9991, 2015.

[10] C.-M. Lai, "Development of a novel bidirectional DC/DC converter topology with high voltage conversion ratio for electric vehicles and DC-microgrids," Energies, vol. 9, no. 6, p. 410, 2016.

[11] J. Moreno, M. E. Ortúzar, and J. W. Dixon, "Energy-management system for a hybrid electric vehicle, using ultracapacitors and neural networks," IEEE transactions on Industrial Electronics, vol. 53, no. 2, pp. 614-623, 2006.

[12] J. Bauman and M. Kazerani, "A comparative study of fuel-cell–battery, fuel-cell–ultracapacitor, and fuel-cell–battery–ultracapacitor vehicles," IEEE Transactions on Vehicular Technology, vol. 57, no. 2, pp. 760-769, 2008.

[13] M. Ehsani, Y. Gao, and A. Emadi, Modern electric, hybrid electric, and fuel cell vehicles: fundamentals, theory, and design. CRC press, 2009.

[14] Z. Haihua and A. M. Khambadkone, "Hybrid modulation for dual active bridge bi-directional converter with extended power range for ultracapacitor application," in Industry Applications Society Annual Meeting, 2008. IAS'08. IEEE, 2008, pp. 1-8: IEEE.

[15] H. Tao, J. L. Duarte, and M. A. Hendrix, "Three-port triple-half-bridge bidirectional converter with zero-voltage switching," IEEE transactions on power electronics, vol. 23, no. 2, pp. 782-792, 2008.

[16] T. Bhattacharya, V. S. Giri, K. Mathew, and L. Umanand, "Multiphase bidirectional flyback converter topology for hybrid electric vehicles," IEEE Transactions on Industrial Electronics, vol. 56, no. 1, pp. 78-84, 2009.

[17] H. Krishnaswami and N. Mohan, "Three-port series-resonant DC–DCconverter to interface renewable energy sources with bidirectional load and energy storage ports," IEEE Transactions on Power Electronics, vol. 24, no. 10, pp. 2289-2297, 2009.

[18] Y.-C. Liu and Y.-M. Chen, "A systematic approach to synthesizing multi-input DC–DC converters," IEEE Transactions on Power Electronics, vol. 24, no. 1, pp. 116-127, 2009.

[19] K. Gummi and M. Ferdowsi, "Double-input dc–dc power electronic converters for electric-drive vehicles—Topology exploration and synthesis using a single-pole triple-throw switch," IEEE Transactions on Industrial Electronics, vol. 57, no. 2, pp. 617-623, 2010.

[20] B. Zhao, Q. Song, and W. Liu, "Power characterization of isolated bidirectional dual-active-bridge DC–DC converter with dual-phase-shift control," IEEE Transactions on Power Electronics, vol. 27, no. 9, pp.
4172-4176, 2012.